INVESTIGATING THE PERFORMANCE OF CUSTOM MANUFACTURED CERMET MOUNTED POINTS WHEN GRINDING TI6AL4V ALLOYS

A.A. ENEVER[1], G.A. OOSTHUIZEN[1], N. SACKS[2,3] M.D. BURGER[1] & J.F. OBERHOLZER[1]

UNIVERSITY OF STELLENBOSCH[1],
UNIVERSITY OF THE WITWATERSRAND[2]
DST-NRF CENTRE OF EXCELLENCE IN STRONG MATERIALS[3]

Abstract

The use and implementation of mounted grinding points in industrial applications are wide spread, ranging from the bio-medical and automotive industries to the aerospace and mining industries. These smaller variants of the larger, more conventional grinding wheels are more affordable to produce, but equally effective in grinding applications. Generally, the abrasive materials implemented in the manufacturing of mounted points do not include the cermet WC-12-wt-%-Co, but rather use alumina- or silicon carbide. This study investigates the use of this WC-12-wt-%-Co cermet as abrasive medium. The resin was varied to manufacture two sets of cermet WC-12-wt-%-Co mounted points that contained 12-wt-% and 16-wt-% resin content, respectively. The grinding performance of these mounted points were evaluated in terms of the tool wear rate, the surface finish and the surface hardening of the Ti6Al4V work piece. The grinding tool wear rate of the 16-wt-% mounted points were more gradual than for the 12-wt-%. The 16-wt-% mounted points produced a smoother surface finish and work hardening occurred on most of the Ti6Al4V work piece surfaces.

Keywords: Grinding, Ti6Al4V, Tool wear, Surface integrity

1. INTRODUCTION

Grinding has been successfully implemented in complex manufacturing processes for the past few decades. It has matured from simple construction stone forming techniques to the modern advanced grinding processes for complex parts being utilized in various industries. The grinding process can be used for large volume material removal or precision geometrical profiling and; even high quality surface polishing.

The common abrasives utilized in the manufacturing of grinding wheels consists of aluminium oxide (alumina) and silicon carbide, while more specialized grinding wheels are made to contain cubic boron nitride and synthetic diamond. The use of tungsten carbide, a ceramic metal (cermet), as abrasive medium for grinding wheel production is not a normal practice.

This study evaluates the manufacturing and performance of tungsten carbide cermet as an abrasive medium in grinding wheels. The grinding wheel design used is that of mounted points, which is a smaller grinding wheel variant. The mounted points are also an economically viable replacement since it requires less abrasive and binder to form the wheel shape. To evaluate the effectiveness of the cermet as abrasive medium, a custom produced mounting point containing WC-12-wt-%-Co is used to grind the Ti6Al4V alloy work pieces.

The performance of the mounted points was evaluated based on their wear rate and the resulting surface integrity of the work piece. The surface integrity characteristics include surface roughness and surface hardness.

2. GRINDING Ti6Al4V ALLOYS WITH WC-12-Co CERAMIC METAL

2.1 The Grinding Process

Grinding is the machining process that makes use of geometrically non-defined tool edges to remove material from a workpiece. The tools are referred to as having non-defined edges, because they consist of abrasive particles bonded with a binder in the shape of a wheel or a section of a wheel, to form a grinding wheel. The grinding wheel rotates at very high speeds in order to remove material from, or cut the workpiece with multiple exposed abrasive particles on the periphery of the grinding wheel. There are six main grinding classifications, namely: surface grinding, peripheral grinding, thread grinding, gear grinding, profile grinding and form grinding (Fritz Klocke and Kuchie, 2009). This study focussed only on surface grinding to achieve the experimental results. Figure 1 a) Grinding wheel composition, b) ISO grinding wheel identification number - Adapted from (Fritz Klocke and Kuchie, 2009).

The grinding wheel consists of three components; the abrasives, binder and air gaps (voids). This composition is true for all grinding wheel types, except metallically bonded wheels, which do not have air gaps within its structure (Hou and Komanduri, 2003). The structure of a grinding wheel can be indicated by using the International Organization for Standardization (ISO) standards, which consists of numbers and letters arranged in specific sequence. This sequence defines the grinding wheel's abrasive, binder, abrasive grain size and grade. The grade of a grinding wheel refers to its hardness. Each manufacturer determines wheel hardness in a different way and thus grinding wheels from different manufacturers with the same grade rating might not have the same hardness. Figure 1 a) shows the composition of a grinding wheel and figure 1 b) is an example of the ISO wheel identification system.

The abrasives utilized in grinding wheels are required to have high hardness, sharpness, thermal resistivity and chemical stability. The abrasives used are synthetic in nature, with the most common being: aluminium oxide (A), silicon

carbide (C), cubic boron nitride (B) and synthetic diamond (SD) (Fritz Klocke and Kuchie, 2009). The size of the abrasive grains greatly influences the work efficiency and performance of a grinding wheel for a specific application. Grain size is measured in mesh per inch and ranges from very coarse grains (numeral 8) to super fine grains (numeral 1200). The grain size numeral can be converted to millimetres as seen in table 1 below.

Table 1: Grain mesh size of various classes of grinding wheels– Adapted from (Fritz Klocke and Kuchie, 2009)

Grain size classification	Grain size Numeral	Dimension [mm]	Grain size	Grain size Numeral	Dimension [mm]
Very Coarse	8	2.83-2.0	Fine	90	0.18-0.13
	10	2.38-1.68		100	0.15-0.11
	12	2.0-1.41		120	0.13-0.09
	14	1.68-1.19		150	0.11-0.06
Coarse	16	1.41-1.0		180	0.09-0.05
	20	1.19-0.84		220	0.075-0.045
	24	0.84-0.60	Very fine	240	0.047-0.043
	30	0.71-0.50		280	0.038-0.035
	36	0.60-0.42		320	0.031-0.028
Medium	46	0.42-0.30		400	0.018-0.016
	54	0.35-0.25		500	0.014-0.012
	60	0.30-0.21		600	0.010-0.008
	70	0.25-0.18		800	0.008-0.006
	80	0.21-0.15		1000	0.005-0.004
				1200	0.004-0.003

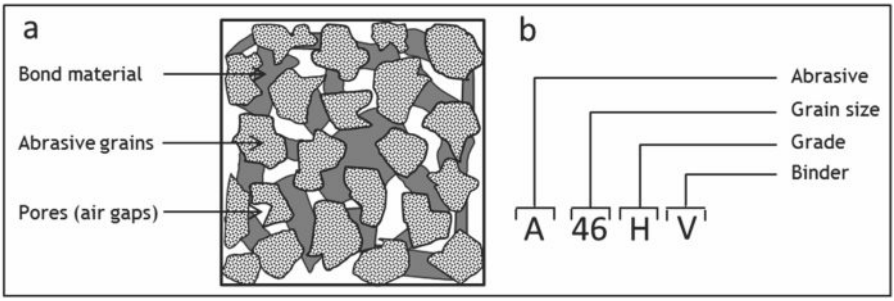

Figure 1: a) Grinding wheel composition, b) ISO grinding wheel identification number - Adapted from (Fritz Klocke and Kuchie, 2009)

The grade of the grinding wheel, as mentioned before, refers to its hardness or how securely the abrasive particles are held together by the binder, and not the hardness of the abrasive particles themselves. The quality of the binder is thus greatly responsible for the hardness of a grinding wheel. The grade scale ranges from A to Z, with A being very soft and Z being very hard. The binders used for grinding wheel production are vitrified (V), resinoid (B), rubber (R) and metallic (M). Vitrified bonded grinding wheels are the most common and are not affected by water, acids, oil or normal temperature variations (Jackson and Mills, 2000). Resin bonded grinding wheels are usually made from phenolic resin, but epoxy resin is also used and should be kept away from chemical exposure. Metallic and rubber binders are mostly used for specialized grinding applications, which is not applicable for this study.

Due to the irregularly shaped grains and their random placing and spacing, the grains can experience three different conditions during operation, namely: cutting, ploughing and sliding. Cutting requires the lowest amount of energy, while the energy requirement for ploughing and sliding is much higher (Hou and Komanduri, 2003). During sliding, frictional heat builds up and is detrimental to workpiece surface integrity. The process of cutting, ploughing and sliding can be seen in figure 2. As the grains become dull, they break away from the binder material, or fractures along a grain fracture line, which produces new sharp grain for cutting. (Klocke, Brinksmeier and Weinert, 2005).

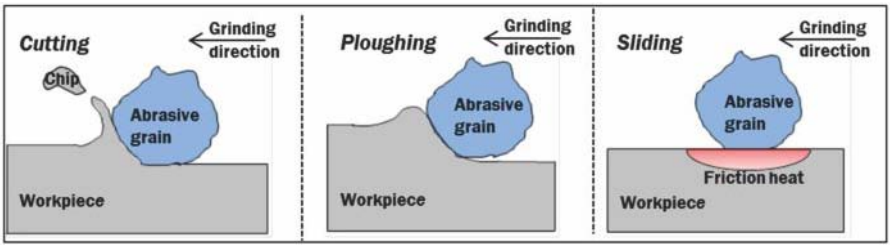

Figure 2: The different effects of the grain conditions on the workpiece surface during grinding – Adapted from (Klocke, Brinksmeier and Weinert, 2005)

The formation of chips during grinding differs greatly to that of a well-defined tool geometry process such as milling. When the grain comes into contact with the work piece material it experiences elastic deformation in that region due to the mostly negative rake angles of the cutting grains (Grote and Antonsson, 2009). As the grain goes deeper into the material, plastic deformation occurs prior to actual chip formation and removal and during this process a large amount of friction and frictional heat is generated. This grinding process can be broken down into several phases as described in figure 3.

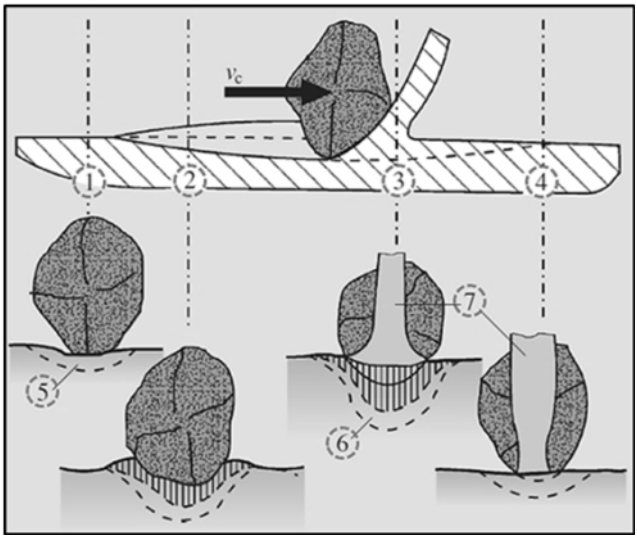

Figure 3: Chip formation phases during grinding: 1) Elastic deformation; 2) Elastic and plastic deformation; 3) Ploughing and shearing of the chip; 5) Zone of elastic deformation; 6) Zone of plastic deformation; 7) Formed chip – Adapted from (Grote and Antonsson, 2009)

The mechanical energy supplied for grinding is almost entirely converted into heat, which mostly flows into the workpiece material while the rest flows into the abrasive grains, binder material and, when present, the cooling lubricant (Batako and Koppal, 2007; Heinzel *et al.,* 2015). The rise in temperature can damage the workpiece material surface by means of the induced residual stresses, cracks and microstructural changes of the material (Oliveira *et al.,* 2015). Figure 4 shows a qualitative heat flow distribution of a single grain. Lubrication during grinding is important to remove frictional heat, but is not implemented in this study.

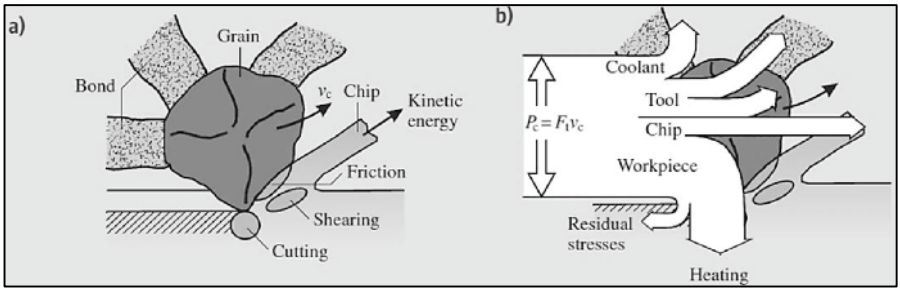

Figure 4: Heat flow and energy distribution in a single grain during grinding: a) Energy conversion; b) heat flow – Adapted from (Oliveira *et al.,* 2015)

Grinding wheel wear can occur as three types of wear; dulling of grains, grain-bond breakage and grain fracturing (Doyle and Turley, 1978). Dulling, or attritious wear, cause flat wear areas on grain edges which leads to increased grinding forces and temperature increases (Malkin and Cook, 1971a). This type of wear usually occurs during gentle grinding conditions, while grain-bond breakage occurs during rougher conditions. Grain-bond breakage wear leads to high volumetric wear due to high grinding loads, leading to constant grinding forces and temperatures (Malkin and Cook, 1971b). Grain fracturing occurs when the stresses within grains are high and the binder does not fail under these stresses (Jackson and Mills, 2000). The grain then fractures along a fracture plane, producing a “new” sharp grain for grinding.

The three main wear mechanisms produce the grinding wheel wear curve seen in figure 5. The first (1) wear region contains the initially sharp grains that undergoes much grain fracturing and corresponds with the break-in period of conventional tool wear. The second (2) wear region has a linear relationship between workpiece material removed and wheel wear and is mostly attritious wear. By the time of the third (3) wear region the grains have become too dull with minimal re-sharpening and the amount of ploughing and rubbing increases relative to cutting.

Grinding wheel wear can occur as three types of wear; dulling of grains, grain-bond breakage and grain fracturing (Doyle and Turley, 1978). Dulling, or attritious wear, cause flat wear areas on grain edges which leads to increased grinding forces and temperature increases (Malkin and Cook, 1971a). This type of wear usually occurs during gentle grinding conditions, while grain-bond breakage occurs during rougher conditions. Grain-bond breakage wear leads to high volumetric wear due to high grinding loads, leading to constant grinding forces and temperatures (Malkin and Cook, 1971b). Grain fracturing occurs when the stresses within grains are high and the binder does not fail under these stresses (Jackson and Mills, 2000). The grain then fractures along a fracture plane, producing a "new" sharp grain for grinding.

The three main wear mechanisms produce the grinding wheel wear curve seen in figure 5. The first (1) wear region contains the initially sharp grains that undergoes much grain fracturing and corresponds with the break-in period of conventional tool wear. The second (2) wear region has a linear relationship between workpiece material removed and wheel wear and is mostly attritious wear. By the time of the third (3) wear region the grains have become too dull with minimal re-sharpening and the amount of ploughing and rubbing increases relative to cutting.

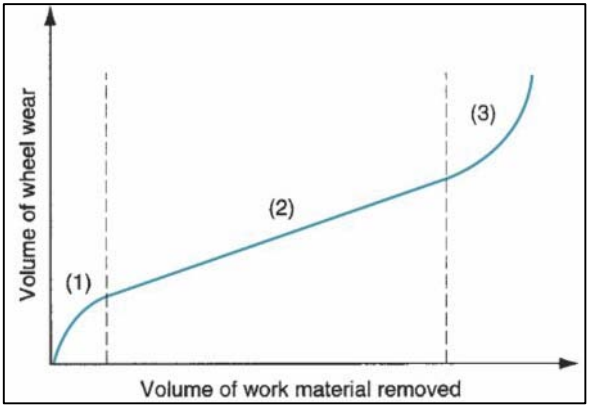

Figure 5: Grinding wheel wear as a function of material removed

2.2 WC-12-wt-%-Co Ceramic Metal

The cermet WC-12-Co consists of tungsten carbide micro particles bonded in a cobalt metal matrix (Saito, Iwabuchi and Shimizu, 2006). The tungsten carbide on its own has high hardness, but is brittle and will fracture under impact loading. The metal cobalt is malleable and has high toughness, but is not very hard. The combination of these two materials creates a unique composite material that inherently has high hardness and toughness (Ferreira *et al.,* 2009). The ratio of the two materials will affect the resulting composite material's mechanical properties of hardness and toughness. A low amount of cobalt will result in a material with low toughness, whereas higher cobalt content will cause the composite material to have low hardness (Picas *et al.,* 2009). The ratio of WC to Co is thus important for the intended application of use (Shetty *et al.,* 1985). For use as abrasive particles, a cobalt content of 12 weight percent is used, providing a good balance between hardness and toughness.

The process of combining these two materials is with a homogenous mixing process in which a ball mill is used to mill powders of the two materials until a uniform particle size is achieved. The homogenous powder mixture can then be further processed into larger parts with a variety of processes. For the

application of grinding wheel abrasive, the WC-12-wt-%Co powder is sprayed with a High Velocity Oxygen-Fuel (HVOF) process in which the temperature is high enough to sinter the cobalt and tungsten carbide, but not to melt the cobalt metal. Large agglomerated particles are formed in the process that can be used as grinding wheel abrasive. The particle size achievable with the HVOF process ranges from 5µm to 600µm, depending on the amount of powder and burning oxy-fuel mixture fed into the spraying process as well as the exit velocity of the agglomerated particles (Silva, Schubert and Lux, 2001).
2.3 Ti6Al4V work piece

The most common titanium alloy used in industry is most certainly the aerospace grade Ti6Al4V variant. This alloy has a unique combination of hardness and toughness, making it an ideal material for the manufacturing of aerospace parts, but also medical implants and automotive parts. A major drawback of the alloy is its operational temperature limit of about 500°C above which oxidation readily occurs, other than its high cost of acquisition (Donachie, 2000; Dimitrov, Conradie and Oosthuizen, 2013).

3. MANUFACTURING OF MOUNTED POINTS

The mounted point design is a combination of the WPL 13-13-06 and WPL 20-10-03 design in accordance with ISO 603-17 standards; having a diameter of 20 mm, a thickness of 13 mm and a spindle shaft diameter of 3 mm, making it better suited for a micro grinding process. This design requires minimal abrasive and binder material (~4.084 cm^3) and is more economical to produce when compared to most common sized grinding wheels (282.74 cm^3 – 1767.14 cm^3). The design of the mounted points can be seen in figure 6.

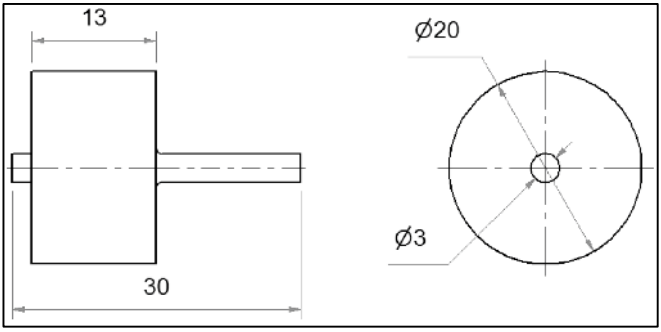

Figure 6: Design drawings for the custom produced mounted points

The abrasive WC-12-wt-%-Co powder used in the study is of the SX408 type, acquired from Global Tungsten and Powders in the USA, and has spherically agglomerated particle geometries. The powder was manufactured with the spray drying process and was analysed post-processing to produce the powder characteristics as shown in table 2.

Table 2: WC-12-wt-%Co powder characteristics

Characteristics	Value
Tungsten content	Balance
Cobalt content	12.1 wt %
Carbon content	5.2 wt %
Iron & other impurities	<1 wt %
Particle size	<31 µm

The binder type chosen for the manufacturing of the mounted points is an epoxy resin. Normally a phenolic resin is used for resinoid type binders, but not exclusively. These two resins have comparable tensile and compressive strengths as well as preparation methods. The differences between the resins are their thermal decomposition temperature threshold and purchase price. Phenolic resin decomposes at a slightly higher temperature than that of epoxy resin. This temperature threshold difference will not have any significant effect on the performance of the mounted points as the temperatures associated with grinding are very high and well above that of both resin temperature thresholds. Epoxy resin is less expensive and easier to acquire than phenolic resin and is thus the reason its use.

The ratio of abrasive particles to the amount of binder is an important parameter in the manufacturing of the mounted points. It has been found that for general application grinding wheels with grain size numeral 100 the resin content should not exceed 30wt% (the minimum is not specified). This grain size is much larger than that to be used in this study and the amount of resin should be determined experimentally. The resin should ideally wet the entirety of the abrasive particles and still be kept to a minimum as not to influence the effectiveness of grinding (Gardziella, Pilato and Knop, 2000).

The optimal resin-to-abrasive ratio has been previously determined to be 12-wt-% and 16-wt-% of the mounted points. This was done by initially determining that the primary loading mode of a grinding wheel is tensile in nature and thus a tensile strength test could be conducted on various resin content samples. The tensile strength test conducted was the Brazilian disk test. From the tensile strength tests the results in figure 7 were produced. A micrograph of the internal structure of samples containing 12-wt-% and 16-wt-% resin content can be seen in Figure 8 (Enever, 2016).

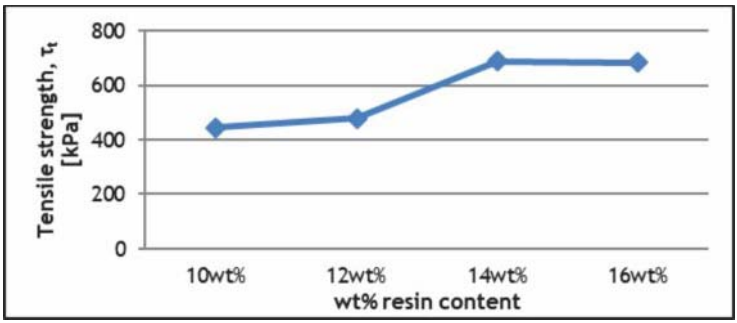

Figure 7: Tensile stress results for various resin content test specimens – Adapted from (Enever, 2016)

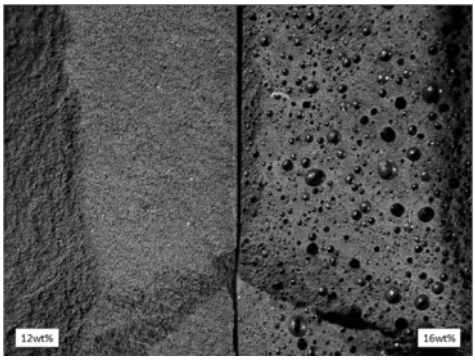

Figure 8: Internal structure of samples with the chosen resin contents

The 12-wt-% resin content was chosen for its low resin content, but greater strength than that of the 10-wt-% resin content. The 16-wt-% resin content was chosen for its strength and produced internal structure. The produced air bubbles, as can be seen in figure 8, are expected to assist in the removal of grinded material as well as cooling of the mounted points. The mounted points are manufactured with the use of a mould. The resin and abrasive is mixed in the required quantities and placed in the mould to cure in the designed mounted point shape. The curing process consists of an ambient room temperature curing phase of roughly 24 hours followed by an elevated thermal curing phase for a total of 9 hours. The mould is modular and can be taken apart in order to remove the mounted points after curing. Figure 9 shows the mould with its components during the resin curing process.

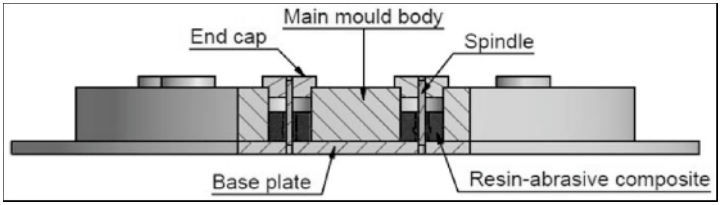

Figure 9: Mounted point mould design with cross section indicating positions of components – Adapted from (Enever, 2016)

4. EXPERIMENTAL SETUP AND DESIGN

The effects of grinding on the custom manufactured mounted points are determined by subjecting the mounted points to a grinding process of the Ti6Al4V alloy. This is done using a micro-CNC machine to perform a micro-grinding process with the manufactured mounted points. The micro-grinding process entails that the work piece material is grinded in such a way as to remove only a small amount of material with every grinding pass. The mounted point will be moved along the face of the work piece material while the grinding depth (or depth of cut) is kept constant. The geometry of the work piece material and the grinding path of the mounted point is illustrated in figure 10.

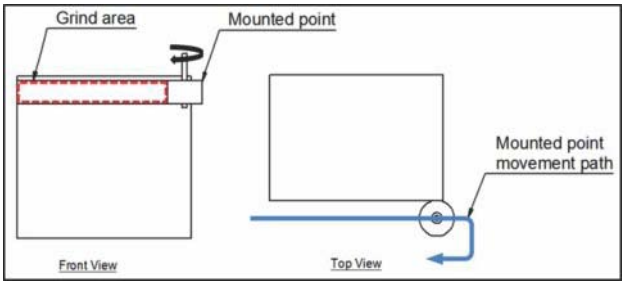

Figure 10: Workpiece geometry and mounted point grinding path

The variables are the resin content (12-wt-% & 16-wt-%), rotational speed (15 000, 17 500 & 20 000 rpm) and transverse feed rate (30, 60 & 90 mm/min), which equate to 18 different grinding combinations.

At each set of parameters a new mounted point is used to ensure that the starting diameter of the mounted points are known (which is based on the mould design). For statistical purposes, each parameter combination set is tested three times with measurements taken between each of the three grinding sets. Table 3 shows the randomized execution order followed during experimentation. The execution number is used consistently throughout the results, discussion and conclusion sections that follows.

Table 3: Grinding parameters and randomized experimental execution order

12-wt-%			16-wt-%		
Execution #	**Spindle speed (RPM)**	**Feed rate [mm/min]**	**Execution #**	**Spindle speed (RPM)**	**Feed rate [mm/min]**
1	20 000	30	**10**	17 500	30
2	20 000	90	**11**	17 500	60
3	17 500	30	**12**	15 000	30
4	17 500	90	**13**	17 500	90
5	15 000	60	**14**	20 000	30
6	17 500	30	**15**	15 000	90
7	17 500	60	**16**	20 000	60
8	20 000	60	**17**	20 000	90
9	15 000	90	**18**	15 000	60

The depth of cut for each grinding iteration is constant at 100 µm, and a final grinding depth of 300 µm would be achieved after three grinding runs. This should ensure that the perpendicular grinding force is kept constant. The transverse grinding force will however change with each set of parameters and could differ for each grinding run due to the various parameter combinations. The grinding length on the work piece was kept constant at 101 mm.

The rotational direction of the mounted points was set up in such a way as to produce an up-grinding grinding process. This process requires less grinding energy and is a more suitable grinding method for a finishing process. The wear of the mounted points was measured using a coordinate measurement machine (CMM) to measure the diameter of circles along the height of the mounted points. The diametric data along with the height of the mounted point was used to calculate the volume of the mounted point. After each grinding run the diameter of the mounted point decreases and; thus the volume. This change in grinding wheel volume was used to indicate the wear rate of the mounted points. The surface finish was measured at the end of the three grinding runs and was measured with a surface profile meter. The surface hardness was also measured at the end of the three grinding runs and is measured with a micro-hardness measuring machine. The location of where surface roughness and surface hardness measurements were taken is shown in figure 11 and 12.

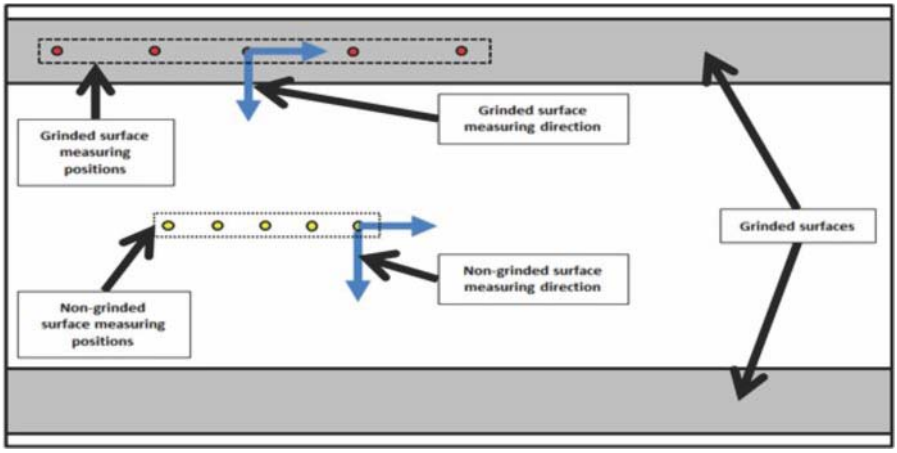

Figure 11: Surface roughness measurement locations (as seen from above)

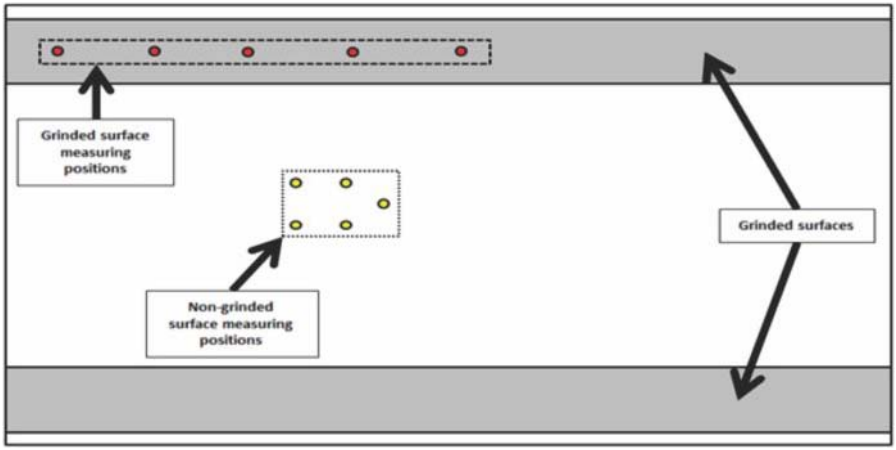

Figure 12: Surface hardness measurement locations (as seen from above)

The rotational power for the grinding process was supplied by a Dremel 4000 high performance rotary tool with a variable speed control of between 5 000 and 35 000 rpm. The power tool has a power rating of 175 W and it is mounted vertically in a micro-CNC machine, so that horizontal grinding can be conducted on the work piece material. The micro-CNC machine is controlled with a computer that executes a G-code describing the required mounted point movement path. The code contains the x-y-z position of the mounted point and the rotational speed is set on the Dremel itself. The work piece is grinded on its four sides with a length of 101mm. This means that per side two sets of experiments can be conducted and eight in total for the four sides. The Ti6Al4V work piece was machined after the eight grinding sets as to allow for

virgin material to be grinded. Figure 13 and 14 shows the experimental setup. The vacuum pipe in figure 13 was used to vacuum the grinding swarf (chips) that were produced during grinding. This was to ensure the air is not polluted with the very fine WC-12-wt-%-Co powder, which could be toxic when inhaled.

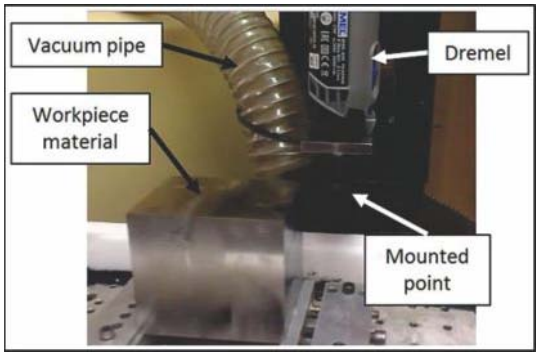

Figure 13: Setup showing the workpiece material, Dremel with clamped mounted point and vacuum pipe

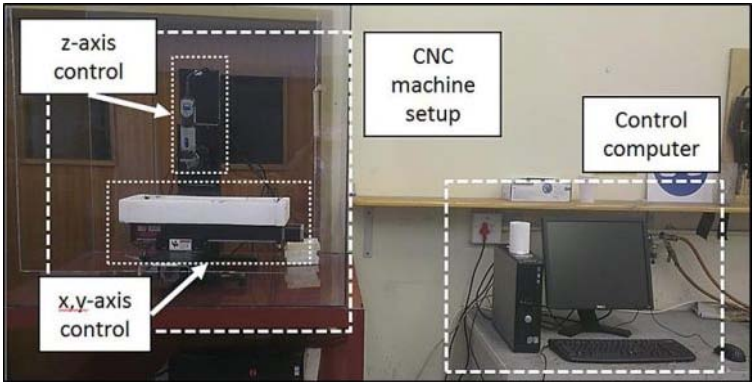

Figure 14: Micro-CNC machine setup with controller computer

It can be noted from figure 14 that the experimentation was conducted within a Perspex box. This was for safety purposes as the amount of energy contained within the rotating mounted points during grinding is significant and could cause much damage as well as injury if the mounted points were to fail catastrophically and break apart. Also, no cooling and/or lubricating fluids were used during experimentation. The use of these fluids might affect the performance characteristics of the mounted points and thus adds another variable to the system. By not using the cooling nor lubricating fluids the measured performance characteristic was purely due to the interaction of the mounted points with the Ti6Al4V work piece material.

5. EXPERIMENTAL RESULTS AND DISCUSSION

The cumulative mounted point wear data was represented on a single graph in terms of grinding runs and not grinding time since the distance was kept constant and not the feed rate for each grinding experimental run. It can subsequently also be represented in terms of total grinding distance. The cumulative wear data for the 12-wt-% resin content mounted points are shown in figure 15. The cumulative wear data for the 16-wt-% resin content mounted points are shown in figure 16.

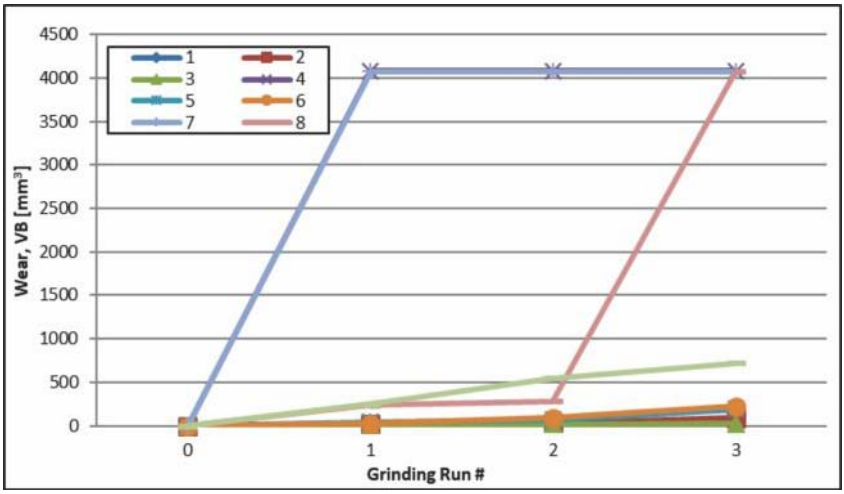

Figure 15: 12-wt-% resin content mounted points cumulative wear data

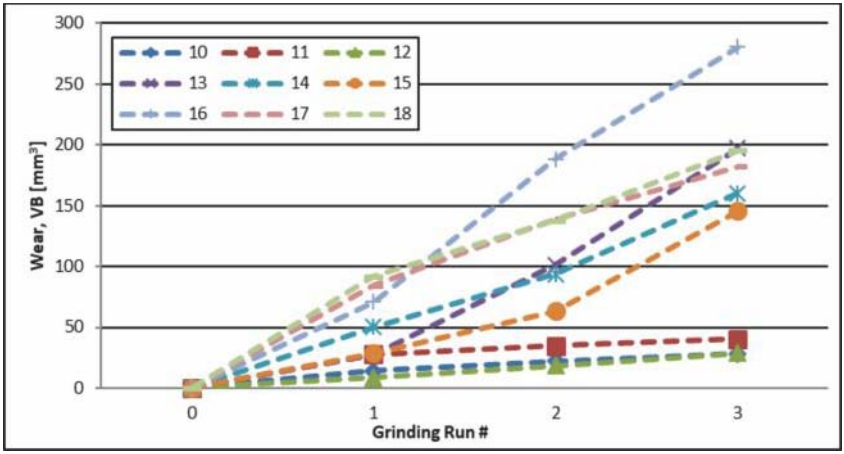

Figure 16: 16-wt-% resin content mounted points cumulative wear data

From these figures it can be seen that mounted point number 4, 7 and 8 failed and recorded 100% wear (all material lost). These three failures could be "flukes" and was discarded. The combined 12-wt-% and 16-wt-% resin content mounted point wear results can be seen in figure 17, which also only shows wear data of below 300 mm^3.

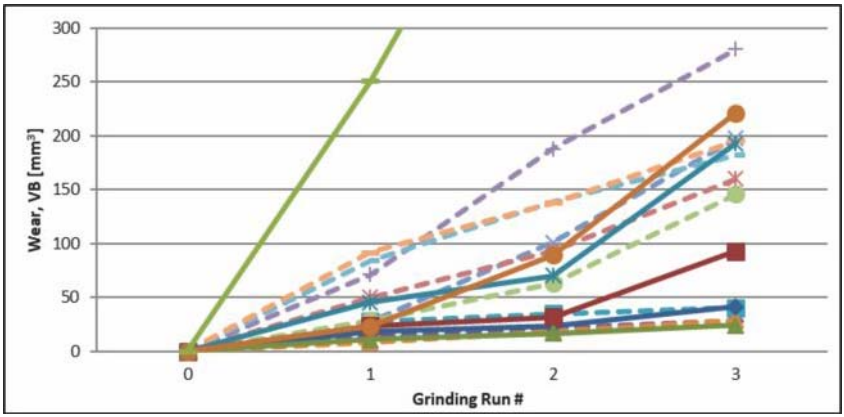

Figure 17: 12-wt-% and 16-wt-% combined cumulative wear results of up to 300 mm^3

The solid lines in figure 17 represent the 12-wt-% mounted points while the dashed lines represent the 16-wt-% mounted points, similarly to figure 15 and 18. It should be noted that the colour of the lines are different between figure 15, 16 and 17. Most of the 12-wt-% mounted points show a drastic increase in wear rate at the third grinding run. The wear rate of the 16-wt-% mounted points was more gradual. The wear rate of the 16-wt-% mounted points seems to be more easily predictable than that of the 12-wt-% mounted points. This assumption can however not be confirmed from these results and further experimentation was required.

The mounted points are designed to remove a small amount of material in a micro grinding process. This process should ideally produce a surface finish that was smooth, but not polished. The grinded area should have a surface roughness less than that of areas not grinded. The surface roughness data is shown in figure 18 as measured with the surface profile meter.

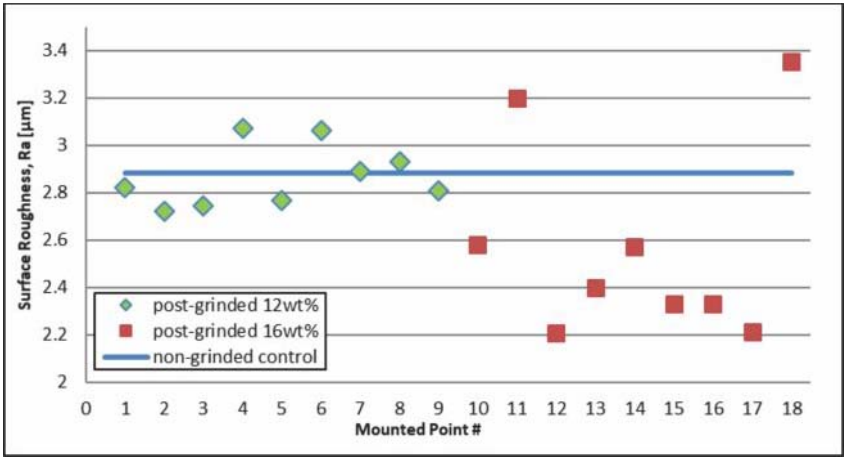

Figure 18: Surface roughness measurement data for the post-grinded workpiece surface

From the data in figure 18 it can be seen that the post-grinded surface roughness produced by most mounted points are well below the pre-grinded roughness. The blue line represents the average surface roughness of the Ti6Al4V work piece over areas where grinding has not taken place and as produced by a face milling operation. The green diamonds are the 12-wt-% mounted points and the red squares the 16-wt-% mounted points. It is also more apparent that the 16-wt-% mounted points produced a smoother surface finish than the 12-wt-% mounted points. This could be due to the increased amount of resin present in the mounted points which helps to produce a better surface finish. The effect of resin content should thus be considered for future studies. Another possibility for the variation in surface roughness could be due to deflection of the grinding system, vibrations and chattering, grinding parameter combinations or mounted point defects. The specific cause can only be identified with further testing and analysis.

The effect of work hardening was expected during grinding due to the elevated temperatures and pressures inherent in the process. The stresses caused by the temperature and pressure increase on specifically the surface being grinded can produce residual stresses post-grinding. These stresses cause the surface hardness of the work piece to be greater than that deeper into the material. The hardness of the grinded surface and non-grinded surface was measured using a Vickers micro-harness indentation tester with a load of 1 kg. The resulting surface hardness can be seen in figure 19.

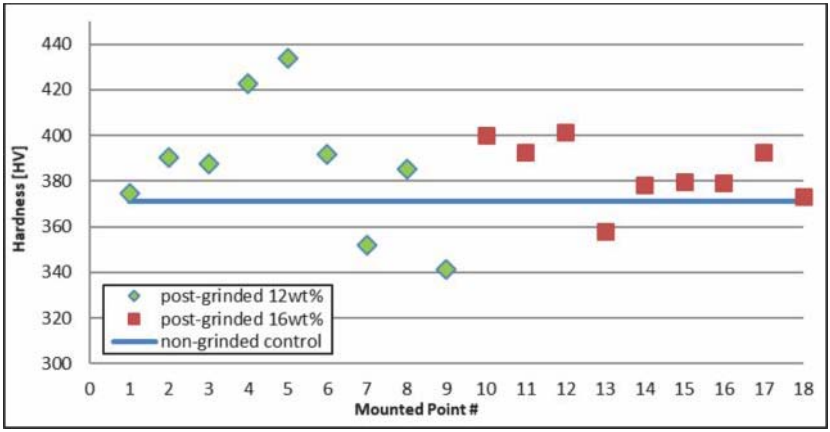

Figure 19: Surface hardness measurement data for the post-grinded workpiece surface

From the data in figure 19 it can clearly be seen that the surface hardness increased after grinding. The results depicted in the figure is purely to indicate that work piece hardening occurs during the grinding process.

6. CONCLUSION

Custom mounted grinding points containing WC-12-wt-%Co as abrasive and epoxy resin as binder was manufactured. The resin was varied to produce two sets of mounted points that contained 12-wt-% and 16-wt-% resin content respectively. The performance of these custom manufactured cermet mounted points were investigated when grinding Ti6Al4V alloys.

The spindle speed and transverse feed rate werew varied, while the depth of cut was kept constant when evaluating the tool wear rate, the surface finish of the Ti6Al4V work piece and associated surface hardening. The wear rate of the 16-wt-% mounted points was more gradual and predictable than for the 12-wt-%. The 16-wt-% mounted points produced a smoother surface finish than the 12-wt-% mounted points. Work hardening also occurred on the work piece surfaces.

The mounted points containing the abrasive WC-12-wt-%Co and particle size of less than 31 µm can be implemented in an intermediate micro-grinding process of components, as this micro-grinding process is intended for minimal material removal and high geometrical accuracy. Future research is required to optimise the use of the abrasive in terms of particle size, particle shape, binder type and amount of binder to be used.

7. REFERENCES

Batako, A.D.L. and Koppal, S. (2007) 'Process monitoring in high efficiency deep grinding- HEDG', *Journal of Physics: Conference Series.* IOP Publishing, 76(1), p. 12061. doi: 10.1088/1742-6596/76/1/012061.

Dimitrov, D., Conradie, P. and Oosthuizen, G. (2013) 'A process planning framework for milling of titanium alloys'. Available at: https://ujcontent.uj.ac.za/vital/access/services/Download/uj:4949/CONTENT1 (Accessed: 11 December 2017).

Donachie, M.J. (2000) *Titanium: a technical guide.* ASM International. Available at: https://books.google.co.za/books?id=HgzukknbNGAC&dq=M.+J.+Donachie,+Titanium:+a+technical+guide,+2nd+ed.+ASM+International,+2000.&lr=&source=gbs_navlinks_s (Accessed: 11 December 2017).

Doyle, E. D. and Turley, D. M. (1978) 'Delamination effects in grinding', *Wear.* Elsevier, 51(2), pp. 269–278. doi: 10.1016/0043-1648(78)90265-X.

Enever, A. (2016) 'Performance evaluation of WC-12wt% Co as grinding wheel abrasive material by machining a titanium alloy'. Available at: http://scholar.sun.ac.za/handle/10019.1/98569 (Accessed: 11 December 2017).

Ferreira, J.A.M. *et al.* (2009) 'A study on the mechanical behaviour of WC/Co hardmetals', *International Journal of Refractory Metals and Hard Materials.* Elsevier, 27(1), pp. 1–8. doi: 10.1016/J.IJRMHM.2008.01.013.

Fritz Klocke, E.H. and Kuchie, A. (2009) 'Grinding', in. Springer, Berlin, Heidelberg, pp. 1–166. doi: 10.1007/978-3-540-92259-9_6.

Gardziella, A. (Arno), Pilato, L. (Louis) and Knop, A. (Andre) (2000) *Phenolic resins: chemistry, applications, standardization, safety, and ecology.* Available at: https://books.google.co.za/books?id=NsvyCAAAQBAJ&dq=A.+Gardziella,+L.+A.+Pilato,+and+A.+Knop,+Phenolic+Resins+-+Chemistry,+Applications,+Standardization,+Safety+and+Ecology,+2nd+ed.+Heidelberg:+Springer,+2000&lr=&source=gbs_navlinks_s (Accessed: 11 December 2017).

Grote, K.-H. and Antonsson, E.K. (2009) *Springer handbook of mechanical engineering.* Springer. Available at: https://books.google.co.za/books?id=9T5kd-ewRE8C&dq=K.-H.+Grote+and+E.+K.+Antonsson,+Springer+Handbook+of+Mechanical+Engineering.+New+York:+Springer,+2009&lr=&source=gbs_navlinks_s (Accessed: 11 December 2017).

Heinzel, C. *et al.* (2015) 'Advanced approach for a demand-oriented fluid supply in grinding', *CIRP Annals.* Elsevier, 64(1), pp. 333–336. doi: 10.1016/J.CIRP.2015.04.009.

Hou, Z. B. and Komanduri, R. (2003) 'On the mechanics of the grinding process – Part I. Stochastic nature of the grinding process', *International Journal of Machine Tools and Manufacture.* Pergamon, 43(15), pp. 1579–1593. doi: 10.1016/S0890-6955(03)00186-X.

Jackson, M. . and Mills, B. (2000) 'Materials selection applied to vitrified alumina & CBN grinding wheels', *Journal of Materials Processing Technology.* Elsevier, 108(1), pp. 114–124. doi: 10.1016/S0924-0136(00)00829-3.

Klocke, F., Brinksmeier, E. and Weinert, K. (2005) 'Capability Profile of Hard Cutting and Grinding Processes', *CIRP Annals.* Elsevier, 54(2), pp. 22–45. doi: 10.1016/S0007-8506(07)60018-3.

Malkin, S. and Cook, N.H. (1971a) 'The Wear of Grinding Wheels: Part 1—Attritious Wear', *Journal of Engineering for Industry.* American Society of Mechanical Engineers, 93(4), p. 1120. doi: 10.1115/1.3428051.

Malkin, S. and Cook, N. H. (1971b) 'The Wear of Grinding Wheels: Part 2—Fracture Wear', *Journal of Engineering for Industry.* American Society of Mechanical Engineers, 93(4), p. 1129. doi: 10.1115/1.3428052.

Oliveira, J.F.G. *et al.* (2015) 'Dry grinding process with workpiece pre-cooling', *CIRP Annals.* Elsevier, 64(1), pp. 329–332. doi: 10.1016/J.CIRP.2015.04.098.

Picas, J.A. *et al.* (2009) 'Microstructure and wear resistance of WC–Co by three consolidation processing techniques', *International Journal of Refractory Metals and Hard Materials.* Elsevier, 27(2), pp. 344–349. doi: 10.1016/J.IJRMHM.2008.07.002.

Saito, H., Iwabuchi, A. and Shimizu, T. (2006) 'Effects of Co content and WC grain size on wear of WC cemented carbide', *Wear.* Elsevier, 261(2), pp. 126–132. doi: 10.1016/J.WEAR.2005.09.034.

Shetty, D K. e*t al.* (1985) 'Indentation fracture of WC-Co cermets', *Journal of Materials Science.* Kluwer Academic Publishers, 20(5), pp. 1873–1882. doi: 10.1007/BF00555296.

Silva, A.G.P. da, Schubert, W.D. and Lux, B. (2001) 'The role of the binder phase in the WC-Co sintering', *Materials Research.* Materials Research, 4(2), pp. 59–62. doi: 10.1590/S1516-14392001000200003.